REVISTA Fitos®

ARTIGO DE PESQUISA

Mechanistic insights into the antiviral effects of curcumin and piperine against Hepatitis C virus: a study of their bioactive properties in hepatocarcinoma cells

https://doi.org/10.32712/2446-4775.2025.1813

Lopes, Rute[1,2]
https://orcid.org/0000-0002-7634-741X

Gaspar, Ana Maria Minarelli[1]
https://orcid.org/0000-0002-7168-9971

Toledo, Lorrane Davi Brito de[2*]
https://orcid.org/0000-0003-3736-4871

Costa, Paulo Inácio da[2*]
https://orcid.org/0000-0002-3350-8308

Rodrigues, Elisandra Márcia[2]
https://orcid.org/0000-0002-1609-2507

[1]São Paulo State University (UNESP), Institute of Chemistry, Rua Prof. Francisco Degni, 55, Quitandinha, CEP 14800-060, Araraquara, SP, Brazil.

[2]São Paulo State University (UNESP), School of Pharmaceutical Sciences, Rodovia Araraquara Jaú, Km 01, s/n, *Campus* Ville, CEP 14800-903, Araraquara, SP, Brazil.

*Correspondence: lorranedbrito@gmail.com; paulo-inacio.costa@unesp.br.

Abstract

Natural bioactive compounds (NBCs) has been reported to possess antiviral and hepatoprotective effects, like curcumin (CL) and piperine (PP). Herein, we report a study of hepatitis C virus biosynthesis and its molecular mechanisms in human hepatocarcinoma cells, expressing or not the HCV (SGR-JFH1) when exposed to CL, PP and its association (CL/PP). Inhibiting concentration (IC50) to CL were 30,95 ± 1,05 µM for Huh-7.5 and 41,96 ± 1,02 µM for SGR-JFH1 cells. For PP, the IC50 were 165,4 ± 1,15 and 200,3 ± 1,05 µM for Huh-7.5 and SGR-JFH1, respectively. An decrease in Cl/PP IC50 were observed with 26,02 ± 1,05 µM for Huh-7.5 and 19,74 ± 1,02 µM for SGR-JFH1. CL and PP induced inhibition of apoptosis. CL treatment at IC20 caused a slight increase of AMPK-α phosphorylation pathway in SGR-JFH1. Caspase-3 was expressed in IC10, and the other pathways were inhibited. HCV cells exposed to PP showed stimulated phosphorylation of FoxO-3a, as well as of the Bax/Bcl-2 in both NBC concentrations. In the CL/PP treatment, the phosphorylation of Akt1 and the Bax/Bcl-2 were shown to be intensified in SGR-JFH1. This work provides a new insight to the control of hepatitis C, when exposure to CL and PP.

Keywords: Hepatitis C. Virus. Curcumin. Piperine.

Introduction

Hepatitis C is a chronic inflammatory disease amongst the major viral hepatitis due to its worldwide distribution and significant public health damage. The World Health Organization (WHO) estimates that in 2019 chronic hepatitis C affected 58 million people[1]. The global prevalence of the disease was 1% of the population, with the number of newly infected people (1.5 million) exceeding the number of deaths (290,000) directly related to liver complications from chronic disease[2].

HCV infection can be acute, progressing to spontaneous cure, in 15 to 45% of cases during the first 6 months of infection. The other 55 to 85% progress to chronicity. Of these, 5 to 20% develop cirrhosis within 30 years, and 1 to 5% die as a result of the disease, from cirrhosis or liver cancer[3]. Coinfection with another virus of a similar contamination route, such as HIV and HBV, may characterize more accelerated disease progression[4,5].

The prevention of the disease is essential to reduce the levels of infection, which includes the treatment of infected individuals, the rapid diagnosis of the disease, awareness, and monitoring of groups with greater vulnerability[6].

Natural bioactive compounds (NBCs) are a class of natural products, derived from isolated nutrients, dietary supplements, and diets to genetically engineered ‘‘designer’’ foods, herbal products, and processed foods, such as cereals, soups, and beverages[7]. Research on bioactive compounds (NBCs) has resulted in products with diverse biological activity, including antiviral and hepatoprotective activity[8].

Curcumin (diferuloylmethane) is a yellow pigment derived from *Curcuma longa* L. (turmeric); which is largely used as a coloring agent and dietary spice[9]. A wide range of protective effects against metabolic disturbances associated with diabetes mellitus, psoriasis, rheumatoid arthritis, Alzheimer, inflammatory bowel, respiratory diseases, hepatic disorders and cancer have been attributed to curcumin[9,10].

The inhibitory effect of curcumin encompasses diverse microorganisms, such as bacteria, fungi, parasites, and viruses, including HCV, HBV, and HIV. The mechanism of action; however, is not the same in all cases. Curcumin can inhibit cell signaling at different steps, in some cases acting directly on the viral replication machinery, reducing the activity of enzymes or even degrading specific proteins[11]. The low bioavailability and rapid degradation in the bloodstream are obstacles in the therapeutic effect of curcumin and, therefore, several strategies have been studied to potentiate its action, such as the use of nanocapsule formulations, liposomes, phospholipid complexes, or combined with other polyphenols, such as piperine[12-14].

Piperine is an alkaloid extracted from pepper (*Piper nigrum L., Piper longum L.*)[15,16], that exhibits various biological activities, such as antioxidant, anti-inflammatory, antidepressant, antimutagenic, antipyretic, antitumor, and antiproliferative properties[16,17].

Several studies have combined the administration of piperine and curcumin, to improve bioavailability and absorption[18-20].

Herein, we report a study of the final stages of hepatitis C virus biosynthesis concomitant with cellular lipid metabolism associated with the formation and secretion of viral lipoparticles, and analyze the molecular mechanisms in cultures from human hepatocarcinoma, expressing or not the HCV subgenomic replicon, SGR-JFH1, when submitted to treatments with the NBCs curcumin, piperine and its association.

Experimental

Material and reagents

Curcumin (CL / C1386), piperine (PP / P49007) and most chemicals were obtained from Sigma-Aldrich, St. Louis, U.S.A. CL and PP were dissolved in dimethyl sulfoxide (1:10) (DMSO; Sigma-Aldrich) and stored at −20°C.

Cells culture and virus

The human hepatocellular carcinoma cell line (Huh-7.5) was obtained from Apath L.L.C. 1590 and 1591 (APP1022 pSGR-JFH1). The Huh 7.5 cells was cultured in Dulbecco's modifed Eagle's medium (Sigma-Aldrich, D1152) supplemented with 10% fetal bovine serum, 10,000 IU/mL penicillin, 10 mg/mL streptomycin, and 1% (v/v) non-essential amino acids (Sigma-Aldrich, M7145). Huh-7.5 expressing the Hepatitis C subgenomic replicon SGR-JFH1 (genotype 2a) was cultured in DMEM supplemented with 500 µg/mL G418 (Gibco, Life Technologies, Grand Island, NY, USA), 11811031). The cells were maintained under 5% CO_2 in 95% humidified atmosphere at 37°C until confluency.

Cell viability

Cell viability rate was determined by 3-(4,5- dimethylthiazol)-2,5-diphenyltetrazolium bromide (MTT). For this assay, Huh-7.5 and SGR-JFH1 cells were plated in 96-well plates (2.5×10^5 cells per well). The cells were exposed to different concentrations of curcumin, piperine (400 to 1,56 µM), and the combination of both (3:1; 6:1; 1:3 and 20:1; proportion), at 37°C overnight. The dilution selected for the subsequent test was 20:1. After 24 h, the culture medium was changed to 100 µL of MTT solution (2 mg/mL in DMEM) and the cells were further incubated for 3 h. The medium was removed, and the purple formazan crystals were dissolved by adding 100 µL DMSO in a shaker for 5 min. The optical density was measured at 490/630 nm using an automated microplate reader. Cell viability was calculated considering non-treated cells as the negative control. All experiments were repeated three times.

Quantitative real-time polymerase chain reaction

HCV RNA quantification was performed in SGR-JFH1 cells (2.0×10^4 cells mL^{-1}, 1 mL/well), without and after treatment with the NBCs or control, for the transcription rate determination and to evaluate the potential of viral replication inhibition by the compounds. In this assay, the RNA was extracted from cells using magnetic microparticles (Abbott Molecular), according to the instructions provided by the supplier.

The HCV target sequence is the 5' UTR region of the genomic RNA, which is specific and highly conserved, and the Abbott proprietary primers were designed to hybridize to this region preventing divergence between genotypes 1, 2, 3, 4, 5, and 6. The Internal Control consists of an RNA sequence unrelated to the HCV target sequence, obtained from the hydroxypyruvate reductase gene of pumpkin (*Cucurbita pepo* - Abbott Molecular).

A calibration curve is required and is constructed by logging the HCV concentration versus the cycle threshold (CT) for the quantification of HCV RNA in samples and controls. At each analysis, high, low and positive controls were also included for process validation.

The levels of target gene expression for each sample group were calculated with the ΔΔCt method compared to control (serum-free medium).

Untreated Cells

This study was performed to determine the amount of viral RNA present in the supernatant of the SGR-JFH1 cell culture over 10 up to days, measured in log international units per mL (log IU mL^{-1}). For this, SGR-JFH1 cells were plated in DMEM-C with G418 at a concentration of 2.0×10^4 cells mL^{-1} (1 mL/well), in a 24-well cell culture plate, incubated in an incubator at 37°C and 5% CO_2 for periods of 3 h, 1, 3, 5, 7, and 10 days. After the incubation, the supernatant was collected and stored in microtubes at -80°C until the viral RNA extraction and amplification step.

MTTP activity by fluorescence

The microsomal triglyceride transfer protein (MTTP) activity assay is based on the use of fluorescence donor and acceptor substrates that allow the detection of MTTP-mediated transfer of neutral lipids, which results in an increased fluorescence intensity. The MTTP activity kit (Sigma-Aldrich, MAK110) was used to prepare suspensions of Huh-7.5 and SGR-JFH1 cells in 24-well flat-bottomed cell culture plates containing 1×10^6 cells mL^{-1} (500 µL/well). The plates were initially incubated at 37°C in a humidified incubator with 5% CO_2 for 24 h. Then, the medium was removed and the cells were treated with the NBCs at 10 or 20 µmol L^{-1} based on the results obtained in viral load quantification and incubated for periods of 1 and 7 days. For vehicle control (VC), cells were exposed to 0.1% (v/v) DMSO in culture medium. Subsequently, the medium was removed and the cells were washed twice with PBS. Then, 150 µL/well of chilled lysis buffer (Tris 10 mmol L^{-1} pH 7.4; NaCl 150 mmol L^{-1}; 1 mmol L^{-1} EDTA, and the protease inhibitors phenylmethanesulfonyl fluoride (PMSF) 100 mmol L^{-1} and leupeptin 1 mg mL^{-1}) were added. Cells were lysed in a Vibra-Cell sonicator (Sonics & Materials, Inc., Connecticut, USA) for 3 cycles of 5 s, on ice, and total proteins were quantified by the Bradford method.

The standard curve for the MTTP activity assay was prepared using 5 µL of fluorescence donor particle in isopropanol at serial dilution (1:2), 100 µL/well, with excitation at 465 nm and emission at 535 nm.

Cell lysate samples after treatment with NBCs were prepared by incubating 100 µg of total cellular protein in 4 µL of donor particle and 4 µL of acceptor particle, 182 µL of assay buffer (from the kit), in a final volume of 200 µL, in a black plate, and incubated at 37°C for 9 h. The fluorescence signal was measured according to the same parameters as above, in a spectrofluorimeter (Biotek Synergy H1, Software-Gen5, Vermont, USA).

Detection of apoptosis by flow cytometry

To assess the effect of NBCs on Huh-7.5 and SGR-JFH1 cells apoptosis, the percentage distribution of living cells, initial apoptosis, late apoptosis or secondary necrosis, and necrotic cell populations was determined by flow cytometry following the methodology of Rieger and colleagues[21] with modifications using an Annexin V detection kit according to the manufacturer's instructions (FITC Annexin V Apoptosis Detection Kit I, BD Biosciences, Pharmingen, San Jose, CA, USA, code 556547). Cells were plated at 1.0×10^6 cells mL^{-1} (500 µL/well), in 24-well plates and incubated at 5% CO_2 and 37°C for 24 h. Then, cells were exposed to the NBCs (10 or 20 µmol L^{-1}) or treated with H_2O_2 (0.1 mmol L^{-1}) as positive control[22], and cells exposed to medium as negative control for 24 h. For this experiment, 100 000 events were analysed for each sample. Analysis were performed on a BD FACSCalibur flow cytometer (BD Biosciences), with data capture using CellQuest Pro 6.0 software, and data analysis with FlowJo version X 10.0.7r2. Readout for annexin V-FITC was performed in channel FL1 (530/30 nm) and for PI in channel FL3 (670 nm).

Western blot analysis

Protein expression and phosphorylation levels was performed by western blotting from the culture of Huh-7. 5 and SGR-JFH1 (5×10^6 cells/well), treated with the NBCs at the calculated concentrations, corresponding to 10% (CI10) and 20% (CI20) inhibitory concentration, in which cell death was observed in only 10 or 20% of the cells and are therefore considered non-cytotoxic, according to ISO 10993-5[23], incubated for 24 h.

To perform the Western blotting experiment, the cell NBCs samples were separated in a 10% SDS– PAGE and transferred to PVDF membrane with transfer system for 2 h 30 min at 40 mA. The blots were exposed to specific primary antibodies: anti-Bcl-2 (code 4223), anti-Bax (2774), anti-Caspase-3 cleaved adjacent to Asp175 (9664), anti-FoxO-3a (12829), anti-FoxO-3a phosphorylated on Ser253 (13129), anti-Akt1 (2938), anti-Akt1 phosphorylated on Ser473 (4051), anti-AMPK-α (5832), anti-AMPK-α phosphorylated on Thr172 (50081), and as an internal control of the constitutive protein anti-GAPDH antibody (2118). For the antibodies produced in rabbit, biotinylated anti-rabbit IgG (H+L) secondary antibody (14709) was used, and for the primary antibody produced in mouse (phosphorylated anti-Akt1) biotinylated anti-mouse (14708) was used, in concentration 1:5000. All these antibodies were purchased from Cell Signaling Technology. After incubation in the primary antibodies, membranes were washed 4 × for 5 min in wash buffer and then incubated in secondary antibody for 24 h under stirring at 4°C. After this period, the membranes were washed again and incubated in avidin-peroxidase conjugate (Abcam AB59653), 1:5000, for 30 min at room temperature under stirring. The reacting bands were detected with a chemiluminescent Western blotting kit (Pierce, Thermo Fisher Scientific, 32106).

Statistical analyses

The assumptions of normality and homoscedasticity were verified using the Statistica 10 program (StatSoft, Inc). Statistical analysis and graphics were performed using GraphPad Prism 5.01 (GraphPad Software, Inc.). The p-value less than or equal to 0.05 was considered statistically significant.

Results and Discussion

Cell viability by MTT assay

The *in vitro* proliferation activity doses of curcumin, piperine or its combination on Huh-7.5 and SGR-JFH1 cells were measured by using MTT assay (**FIGURA 1**). After 24-h incubation with curcumin (CL), IC_{50} values were 30,95 ± 1,05 µM for Huh-7.5 (**FIGURA 1a**) and 41,96 ± 1,02 µM for SGR-JFH1 cell lines (**FIGURA 1d**). For piperine (PP), the IC_{50} were 165,4 ± 1,15 and 200,3 ± 1,05 µM for Huh-7.5 and SGR-JFH1 (**FIGURA 1b and 1e**), respectively. These results corroborated with a previous study which showed in human hepatocellular liver carcinoma (HepG2) cells a significantly lower IC_{50} at 51.7 ± 9.0 µM for acetal-linked nanocarrier conjugated with curcumin[24]. Another study tested the antiproliferative activity of curcumin by MTT assay and discovered that curcumin effectively inhibited the growth of HepG2 cells at 24 h with IC_{50} (23.15 ± 0.37 µmol/l), which was similar to previous studies demonstrating a wide range of growth inhibitory on various cancer cell lines[25]. The addition of curcumin during infection of native Hu-7.5 cells with hepatites C vírus cell-culture-derived HCV (HCVcc) resulted in dose-dependent inhibition of infectivity with no cytotoxic effects with IC_{50} of 8.46 ± 1.27 µM[12]. Prasad and collaborators[26] reported IC_{50} values of spice active principles as piperine for inhibition 5-lipoxygenase enzyme (5-LO) activity of human polymorpho-nuclear

leukocytes (PMNLs) was 54 µM. Complete inhibition of platelet aggregation was observed at IC_{50} (300 µM) of piperine concentration[27]. Our results showed that the curcumin combinated with piperine (CL/PP 20 :1) resulted in decreaed IC_{50} values of 26,02 ± 1,05 µM for Huh-7.5 (Fig. 1c) and 19,74 ± 1,02 µM for SGR-JFH1 culture cells (**FIGURA 1f**). This effect of CL/PP could be relationed with its antioxidant potential. Low oral bioavailability of curcumin has been proposed to limit its approval as a therapeutic agent[28]. Curcumin is among agents whose bioavailability is enhanced by piperine. Piperine proved to increase the bioavailability of curcumin and to potentiate its protective effects against chronic unpredictable stress-induced cognitive impairment and associated oxidative damage in mice[29]. The combination of curcumin and piperine showed strong antioxidant and protective effect against quinolinic acid (QA)-induced behavioral and neurological alteration in rats[30].

FIGURE 1: Dose-dependent cytotoxicity and IC_{50} of natural bioactive compounds (NBCs) on Huh-7.5 (a, b and c) and SGR-JFH1 (d, e and f) cell lines incubated with increasing concentrations (C) of NBCs. Curcumin (CL), Piperine (PP), and Curcumin combinated with piperine (CL/PP 20 :1).

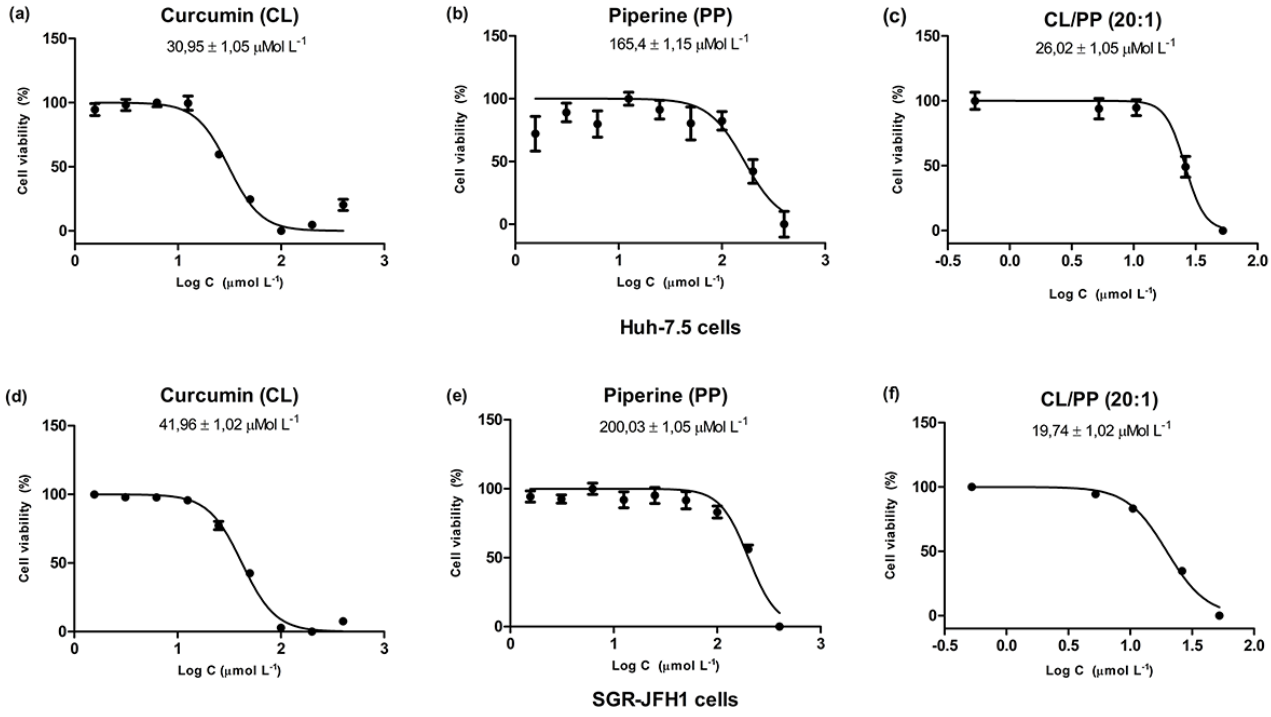

Quantification of viral RNA in SGR-JFH1 cells without treatment

Performance of Real-Time (RT-PCR) assay for quantitation of Hepatitis C virus RNA has been proposed[31,32]. The quantification of viral load in SGR-JFH1 cells without the interference of treatments indicates that HCV replicates significantly when maintained in cell culture (**FIGURE 2**), following the same trend observed in the cell proliferation assay, possibly due to the replicative capacity of the virus, and the increased population of cells, which were not subjected to care of medium exchange or passages by trypsin action in the observed period[33].

FIGURE 2: Quantitative analysis by Real-time PCR (qRT-PCR) assay to determine HCV RNA viral load in supernatant SGR-JFH1 cells after incubation for 3 h, 1, 3, 5, 7, and 10 days.

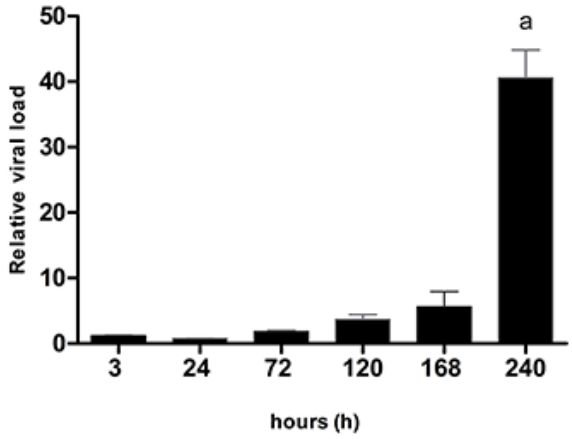

Viral RNA shows a significant difference from day 5 of incubation compared to day 1 and compared to the cell culture bottle supernatant before plating. The increase in viral load occurs steadily and progressively, until approximately day 7 of incubation when the difference becomes pronounced. For this reason, for the subsequent experiments, the maximum analysis period was kept at 7 days of incubation.

Quantification of viral RNA

In this study, RT-PCR assay for quantitation of Hepatitis C virus RNA exposed to NBCs (CL, PP and (CL/PP 20 :1) was performed. It is possible to observe in **FIGURE 3a** that at 1 day of incubation, the treatment with CL/PP among the of 5, 10 and 20 µmol L^{-1} concentrations had inhibition of intracellular viral synthesis, with a viral load index result (mean ± standard deviation) of 0.51 ± 0.08 to VC, while for PP it was 0.58 ± 0.005, but only at 100 µmol L^{-1}. The other treatments showed no inhibitory effects in the intracellular environment. In the supernatant, however, except for PP at 100 µmol L^{-1}, the treatments showed significant performance, with approximately 0.65 ± 0.09 overall average. Only PP at 5 µmol L^{-1} showed a clear difference from several other treatments, due to the relative viral load over twice the control (**FIGURE 3b**).

In **FIGURE 3c**, after 3 days of incubation PP and CL/PP at 5 µmol L^{-1} showed around 0.27 ± 0.16 on average viral load compared to VC in the intracellular environment. At the same time, PP and CL/PP (except PP at 5 µmol L^{-1}) exhibited inhibitory effects at different concentrations, averaging 0.71 ± 0.12, between each other, of viral particles released in the supernatant (**FIGURE 3d**). Thus, in this period, despite having high viral synthesis, these treatments influenced the inhibition of virus release into the extracellular medium.

Regarding the 7 day incubation, the results were very expressive, with inhibition observed in all treatments, both of viral synthesis and release into the supernatant (**FIGURE 3f**). The significant differences were indicated directly in **FIGURE 2e and 2f**, the result observed by the treatment with PP at 100 µmol L^{-1}, with 0.71 ± 0.22 viral load index in the intracellular medium (**FIGURE 3e**), to other treatments that had notable inhibitory effects, PP 10 µmol L^{-1} in intracellular medium, and 10 and 20 µmol L^{-1} in the supernatant, below 0.15.

Except therefore for this result at a higher concentration of PP (100 µmol L^{-1}), the other treatments of the intracellular medium at 7 days of incubation together exhibited a mean viral load index of 0.32 ± 0.19 (**FIGURA 3e**), while in the supernatant this mean was 0.22 ± 0.10 (**FIGURA 3f**). Thus, one can see the

important inhibitory effect that CL, PP, and CL/PP NBCs exerted on HCV viral lipoparticle synthesis and release after longer periods of treatment, with great complementary therapeutic potential, which can be further thoroughly investigated, especially in conjunction with already established therapies.

FIGURE 3: Real-time PCR assay for HCV RNA quantification, with result in viral load index from the ratio treatment per vehicle control (VC), performed in SGR-JFH1 cells after treatment with curcumin (CL), piperine (PP), and curcumin combinated with piperine (CL/PP 20 :1). (a) and (b); (c) and (d); (e) and (f): incubation periods of 1, 3, and 7 days, respectively. The viral load scale was maintained between graphs of results in intracellular environment and supernatant to facilitate comparison.

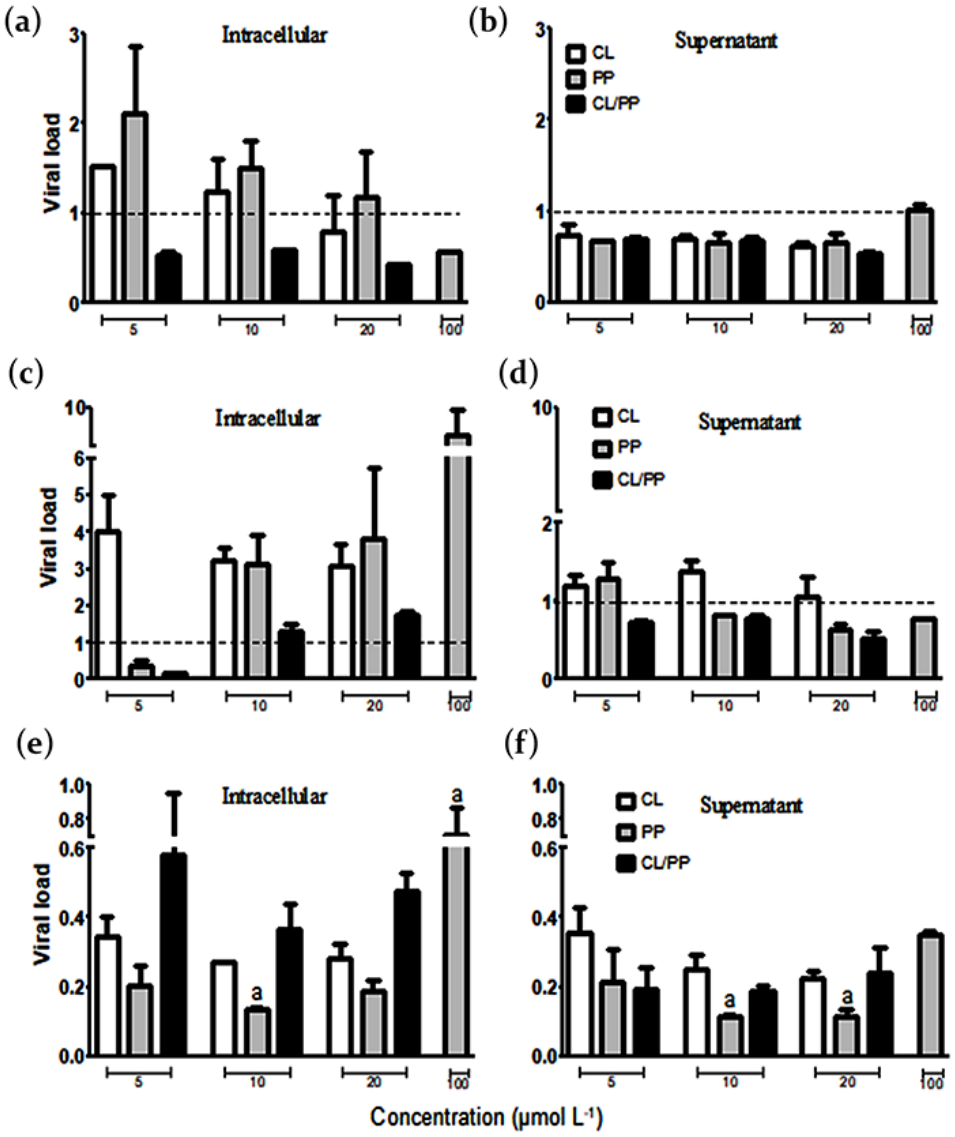

The antiviral effects of CL constitute a relevant bias of study. Kim and co-workers[34] tested CL activity in a concentration range of 5 to 15 µmol L^{-1} in Huh-7 cells expressing a subgenomic HCV replicon and observed a reduction in luciferase activity of the labeled replicon to approximately 40% relative to control. In another work, a 50% reduction of HCV RNA was observed after treatment with CL at a concentration of 20 µmol L^{-1} in Huh-7.5 cells expressing the subgenomic replicon 1b, tagged with luciferase[35].

Also using CL concentrations from 5 to 20 µmol L^{-1} in the treatment of Huh-7.5 cells expressing different luciferase-labeled HCV genotypes, inhibition of virus entry into the cell, performed by transfection or

electroporation, was demonstrated, however no inhibitory effect was observed in the replication, assembly or release steps[12].

The results obtained in this work are significant, especially considering the observed trend up to 10 days of continuous viral load increase in the qRT-PCR assay without treatments. Evaluating the full duration of the assay, it can be seen that the performance of PP and CL/PP was superior to that of CL alone. Therefore, this observation may be related to the increased bioavailability of CL by the concomitant use of PP, whose results alone were also equally promising and unpublished, considering that so far, no studies analyzing the antiviral effect of PP on HCV have been found in the literature.

The relationship between the bioavailability of CL and its performance has been described by several authors[12-14]. This effect is due to the low solubility in water and is mainly observed in oral administration, considering the complete route of metabolism and absorption of CL[20,36].

MTTP activity

The active enzyme triglyceride transfer protein (MTTP), present in the cell lysate, transfers the neutral fluorophore-labeled lipid substrate from a donor to an acceptor molecule, with photon emission detected as an increase in fluorescence intensity Microsomal triglyceride transfer protein (MTTP) have been attributed to impact lipoprotein as well as lipid secretion and predispose individuals with and without HCV infection to hepatocyte triglyceride accumulation, causing the hepatic steatosis[37-39]. The important role of MTTP in the pathogenesis of fatty liver in hepatitis C has been highlighted. The minor MTTP polymorphism variant rs1800803 was associated with increased steatosis among patients with genotype 3[40,41]. MTTP rs1800591 variant combined with HCV genotype 3 robustly increased the chance of hepatic steatosis[39].

The results obtained in the MTTP activity assay are shown in **FIGURE 4**. It is possible to observe that, at 1 day of incubation (**FIGURA 4a**), there was a significant difference ($p < 0.05$) only between the treatment at 10 µmol L^{-1} with PP in Huh-7.5 cells and the treatment with the same compound at 20 µmol L^{-1} in SGR-JFH1, with stimulated activity in the latter relative to the control. This indicates that, at equal concentrations, the treatments do not significantly alter the enzymatic action, and that the presence of the virus does not cause a significant increase in MTTP activity either.

FIGURE 4: Analysis of MTTP activity in cell lysate of Huh-7.5 and SGR-JFH1 cell lines exposed to curcumin (CL), piperine (PP), and curcumin combinated with piperine (CL/PP 20 :1) with result in relative MTTP activity index, calculated from the fluorescence intensity of each treatment (FIU) to VC (DMSO 0.1%). A: and B: incubation for 1 and 7 days, respectively *p < 0,05.

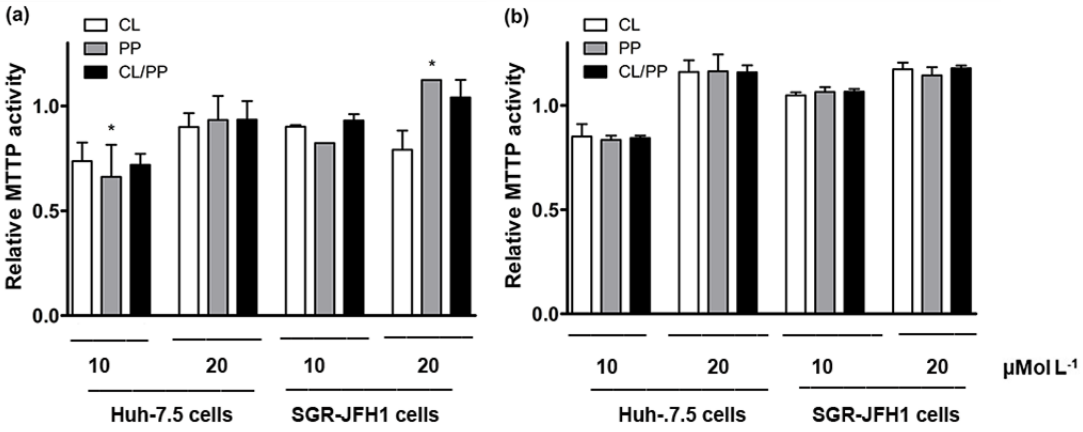

In general, it is possible to see that in Huh-7.5 cells, in 1 day of incubation (**FIGURE 4a**), the enzyme presented activity index (mean ± standard deviation) reduced by the action of CL, PP, and CL/PP in 10 µmol L^{-1} with mean activity of 0.74 ± 0.12; 0.66 ± 0.22 and 0.72 ± 0.07, respectively. In this same period, to a lesser extent, there was also inhibition in the treatments at 20 µmol L^{-1} (0.92 ± 0.10) and, in SGR-JFH1, the treatments at 10 µmol L^{-1} (0.88 ± 0.05), along with CL at 20 µmol L^{-1} (0.79 ± 0.13). After 7 days of incubation (**FIGURE 4b**), inhibition of enzyme activity was observed only in Huh-7.5 cells, for the treatments at 10 µmol L^{-1} (0.84 ± 0.04).

In the 7-day incubation period, a trend towards stimulation of MTTP enzyme activity is perceived in the treatments at 20 µmol L^{-1} in Huh-7.5 cells (**FIGURE 4b**). The overall mean of the results of the treatments with MTTP activity index/control greater than 1 was 1.16 ± 0.06. Consequently, it can be inferred that CL, PP, and CL/PP treatments may facilitate stimulation of MTTP enzyme action under certain conditions.

In regards to the HCV-infected cell, the MTTP activity continues to increase after the treatments, considering that the enzyme is fundamental for the secretion of new viral lipoparticles, and, in this case, the NBCs studied do not exert an immediate inhibitory effect. Therefore, it is possible to infer that the viral load reduction observed previously is not directly related to MTTP activity. $MTTP^{R46G}$ iPSC-derived hepatocytes exhibit, excess intracellular lipid storage, apoB secretion absence, decreased hepatic lipid secretion, and excess intracellular lipid storage, presumably due to loss of MTTP lipid transfer activity[42]. MTTP activity in transfected COS cell plasmids was significantly reduced by the R634C mutation (49.1 nmol/ml vs. 185.8 nmol/ml for mutated and nonmutated MTTP, respectively; P = 0.0012). The difference in activity was not due to lower levels of mRNA in the transfected cells but was rather the result of either lower enzyme activity or reduced protein level[43].

The reduction of the enzymatic activity on the hepatocytes, however, may be of interest in the treatment of dyslipidemias, such as in cases of familial hypercholesterolemia, and could be evaluated for performance in simultaneous employment with other MTTP-inhibiting drugs, such as lomitapide[44], or strategies that include the use of statins, which are HMG-CoAR inhibitors and therefore reduce cholesterol synthesis[45,46].

Apoptosis analysis

The annexin V and propidium iodide (PI) protocol is often used to determine apoptosis, necrosis, or cell viability from the characteristics of plasma membrane integrity and permeability. During the process of apoptosis, one of the first events is the exteriorization of membrane phosphatidylserine, and annexin V shows high affinity for this molecule, allowing the identification of apoptosis at early stages. In necrotic cells, annexin V accesses the entire plasma membrane, because in these cells the membrane is ruptured. PI, in turn, is a nuclear fluorescent dye, which binds to DNA in dead cells or late stages of apoptosis; thus, PI is an exclusionary indicator of cell viability, also used to determine plasma membrane integrity, because in viable cells or early stages of apoptosis, the cell membrane is not permeable to PI[21,47].

FIGURE 5 shows the trend toward inhibition of apoptosis by treatments with NBCs, calculated relative to the vehicle control, with mean ± standard deviation. CL in Huh-7.5 cells mean result was 0.74 ± 0.15 for the concentrations tested. In SGR-JFH1 cells, the trend post-treatment with NBCs was towards apoptosis induction, averaging 1.57 ± 0.50 at levels similar to the death induction control, H_2O_2 (1.81 ± 0.17), except for CL/PP at 10 µmol L^{-1}, which showed similar activity to VC. However, there was no statistically significant

difference between the groups. This result demonstrates that, in the observed period, the treatments did not exert a significant influence on apoptosis in both cell lines.

FIGURE 5: Analysis of the apoptosis index in Huh-7.5 and SGR-JFH1 cells after treatment with curcumin (CL), piperine (PP), and curcumin combinated with piperine (CL/PP 20 :1) in different concentrations (10 µmol L^{-1} and 20 µmol L^{-1}) .

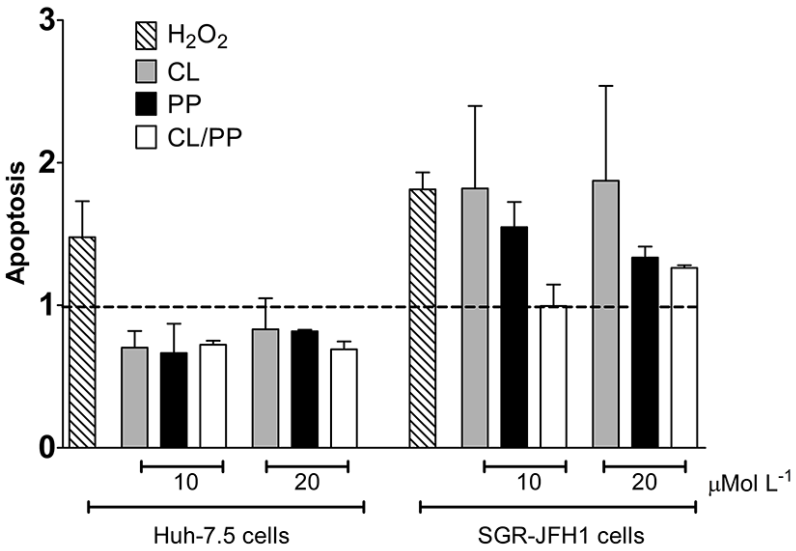

The antitumor activity of CL has been previously described, related to the ability to induce apoptosis in different cell lines, including human leukemia HL-60 cells, human hepatocarcinoma stem cells, and some specific splenocyte subtypes [20,48,49]. This activity is related to interference with various molecular targets, such as in the NF-κB and STAT3 signaling cascade[20]. Shiu and colleagues[50] demonstrated the ability of CL to induce apoptosis and inhibit cell viability in Huh-7 cells, proportional to the dose administered. In this same study, they found that in cells expressing HCV, the viral capsid protein can inhibit the effect of CL on apoptosis induction. Also, the CL showed the viability of preadipocytes was significantly decreased by treatment with 30 µM curcumin, a concentration that caused apoptosis in preadipocytes, and inhibited adipocyte differentiation, leading to suppression of adipogenesis[51].

PP, in turn, was tested in human cervical cancer HeLa (Henrietta Lacks) cells and mitomycin-C-resistant cells (HeLa/MMC) and showed a significant apoptosis-stimulating effect in both strains[52]. Another study reported that piperine could induce p53-mediated cell cycle arrest and apoptosis via activation of caspase-3 and caspase-9 cascades as well as increasing the Bax/Bcl-2 ratio of lung cancer A549 cells[53]. Piperine induced apoptosis in Hep G2 cells resulting in 38% of Annexin V-FITC stained early apoptotic cells and 24% PI stained late apoptotic cells on 48 h of treatment. The essential markers levels of apoptosis such as cleaved caspase 3 and 9 were also remarkably increased in piperine treated cells[54].

Changes in concentrations or incubation time may have exacerbated the effect observed in this experiment, accentuating the trend shown of apoptosis induction in SGR-JFH1 cells. These concentrations were chosen based on the inhibitory effect on viral load. The induction of apoptosis in these cells would be remarkable, considering that the viral machinery uses the cell for its replication and release with subsequent infection of surrounding cells and consequent return to the bloodstream. Even more advantageous would be that this apoptosis-inducing effect in uninfected cells does not replicate,

and this tendency was also observed in Huh-7.5 cells, thus restricting itself to the presence of HCV. Therefore, the use of CL, PP, and the combination CL/PP present a potential to be further explored regarding the effect of inducing apoptosis of HCV-infected cells.

Determination of protein expression levels by western blotting

The concentrations tested for the treatments with the NBCs followed the inhibitory concentration values of 10 and 20% for Huh-7.5 and SGR-JFH1 cells, considering that the purpose of the study was to determinethe effect of the treatments, without cytotoxic effects. **FIGURE 5** shows the images captured by scanning the western blotting membranes, after the chemiluminescent reaction, for the proteins of interest. Some proteins did not show detectable levels by this technique.

FIGURE 6: Effect of CL, PP, and CL/PP on cell signaling protein biomarkers based on the inhibitory concentration IC20 and IC10. The Huh-7.5 and SGR-JFH1 cells were subjected to NBCs up to 24 hours when the samples were collected to allow protein analysis by western blotting. VC: Vehicle control; IC20: Treatment in IC20 inhibitory concentration and IC10: Treatment in IC10 inhibitory concentration. CI = curcumin, PP = piperine, CL/PP = curcumin + piperine.

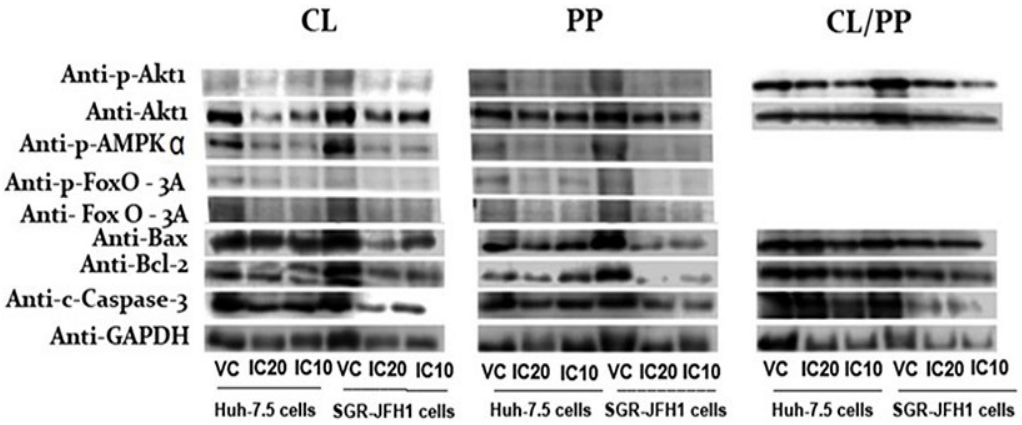

From the obtained results, the CL treatment at IC20 caused a slight increase of AMPK-α phosphorylation pathway in SGR-JFH1 cells compared to cells without the virus (**FIGURE 6**). At the same time, Akt1 phosphorylation, the Bax/Bcl-2 ratio, and the rate of cleaved Caspase-3 were inhibited by the action of this concentration of CL. The phosphorylation of FoxO-3A was slight detected in vehicle control of Huh 7.5 cells. In HCV infection and hepatic steatosis, FoxO-3a is altered, and its expression is believed to be downregulated in some hepatocellular carcinomas. One effect of HCV concerning FoxO-3a is the regulation of the innate immunity signaling pathway, and increased activity levels in cases of malnutrition associated with HCV infection, contributing to insulin resistance and infection persistence[55,56].

As mentioned, CL treatment in Huh 7.5 cells caused an slight detection phosphorylation rate of FoxO-3a in VC sample (**FIGURE 6**). It should be noted, however, that increased nuclear levels may signify increased transcriptional activity, with stimulation of autophagy and gluconeogenesis. In this work, however, the localization of the protein was not determined, which would be interesting to investigate in the future.

In IC10 treatment, only cleaved Caspase-3 was markedly expressed, and the other pathways were inhibited. Finally, phosphorylation of SREBP was detected only in the VC samples, suggesting its inhibition upon CL treatment (**FIGURE 6**).

AMPK functions as an energy sensor in cells, activated in response to a decrease in energy availability, indicated by the ATP/ADP or ADP/AMP ratio, which promotes a change in metabolism to increase catabolism and reduce anabolism by phosphorylating key proteins in several pathways, such as the lipid homeostasis pathway, the glycolytic pathway, and mitochondrial homeostasis (**FIGURE 7**). AMPK also regulates the activation of certain genes related to metabolism, autophagy, and lysosomal function, such as the stimulation of FoxO-3 transcription under energy stress, which results in the activation of autophagy genes[57].

FIGURE 7: The NBCs (CL, PP, and CL/PP) effects in different cell signaling pathways, with responses that may vary according to the concentration employed. Stimulation/inhibition of a specific protein can trigger changes in other pathways; however, in some cases, it is not possible to determine the direct relationship of the treatments' activities in different pathways.

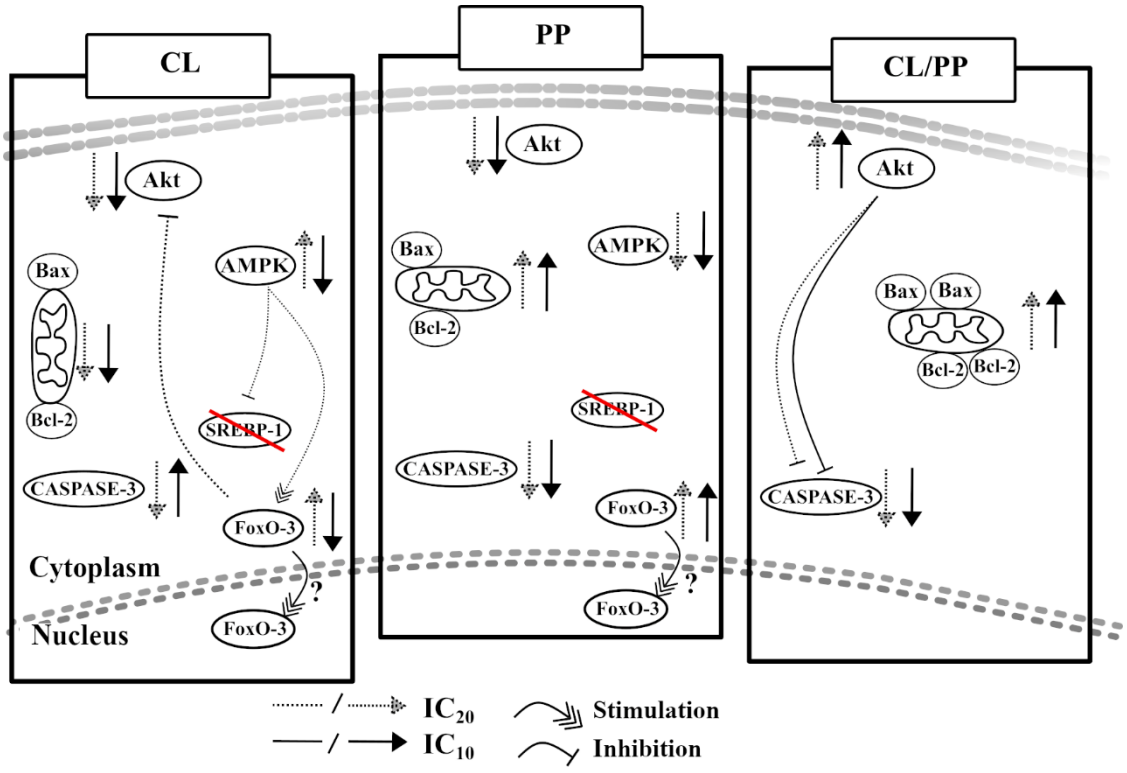

In HCV-infected cells, AMPK phosphorylation is inhibited, while Akt phosphorylation is stimulated[58]. Thus, although subtle, stimulation of AMPK phosphorylation in infected cells may be a useful effect in the treatment of the disease. AMPK activation suppresses lipogenesis and leads to the inactivation of SREBPs in rat hepatocytes[59].

As for caspase-3, stimulated in CL treatment with IC10, common to intrinsic and extrinsic pathways, and considering that the Bax/Bcl-2 ratio is considerably decreased, it can be inferred that, in this case, apoptosis is being initiated by the extrinsic pathway, through cell receptors, possibly due to treatment influence. In patients with chronic hepatitis C responsive to antiviral treatment, an increase in caspase activity and synthesis of pro-apoptotic proteins was observed, directly correlated to virus elimination[60].

Apoptosis is present in physiological and pathological processes, and acts in the regulation of homeostasis in response to various stimuli, reducing the number of cells, and leading to tissue remodeling through cell proliferation. The degree of remodeling varies according to the relationship between apoptosis and proliferation. Bcl-2 is an anti-apoptosis protein that inhibits cell death without affecting proliferation. Thus,

Bcl-2 expression is associated with a favorable prognosis in several malignant tumors. The pro-apoptotic protein Bax is part of the Bcl-2 family, and it is the Bax/Bcl-2 ratio that determines the susceptibility of cells to apoptosis. The main effector enzyme of this process is caspase-3, and its activation can occur by 3 pathways: the intrinsic ones, being the mitochondrial, related to Bax and Bcl-2; or that of the endoplasmic reticulum, or by the extrinsic pathway, through death receptors (FAS, FAS-L)[61,62]. Expression of the viral capsid and E1/E2 proteins, as well as continuous HCV genomic RNA replication, initiate apoptosis. The capsid protein induces the activation of caspases-8 and -9 (initiators), with subsequent activation of caspase-3 (effector), which triggers DNA fragmentation and cell death[63].

PP treatment in HCV cells showed stimulated phosphorylation of FoxO-3a, as well as of the Bax/Bcl-2 in both tested NBC concentrations, while the other proteins Akt1, AMPK-α and Caspase-3, showed inhibited or undetectable post-treatment, relative to uninfected cells (**FIGURE 5**). In a study with human ovarian adenocarcinoma cells (SK-OV-3), the use of paclitaxel combined with piperine resulted in increased Bax and Caspase-3, with decreased Bcl-2. It has been suggested that this effect, of inducing apoptosis by the intrinsic pathway, is related to antiproliferative activity, induction of cell cycle arrest, and programmed cell death, in various tumor cell lines[64]. In contrast, in CL/PP treatment several proteins were not detected by this technique (**FIGURE 6**). In any case, the phosphorylation of Akt1 and the Bax/Bcl-2 ratio were shown to be intensified in cells with the virus, while cleaved Caspase-3 was inhibited (**FIGURE 6**).

As for its function, the Akt protein has more than 100 substrates with diverse downstream regulatory effects, which belong to the different functional classes, such as transcription factors, lipid and protein kinases, metabolic enzymes, cell cycle regulators, and others[65]. The interaction between viral and cellular proteins, with consequent activation of the PI3K/Akt pathway, facilitates viral entry and replication, in HCV infection[66,67]. In addition, Akt is a proto-oncogene activated in various types of cancer, which acts as an anti-apoptotic factor upon various stimuli, such as radiation, hypoxia, and chemotherapy[68]. Therefore, it is difficult to determine whether CL/PP treatment could show beneficial or detrimental effects in HCV treatment, considering the two activated pathways, which act divergently in the regulation of apoptosis.

Conclusion

This study examined the mechanisms by which the NBCs curcumin, piperine, and its association acts on HCV infection to different biological effects. Longer period of NBCs exposure resulted in a more pronounced reduction on HCV viral RNA replication. There was a tendency to induce apoptosis after NBCS treatment in infected cells, suggesting a pro-apoptotic effect of NBCs. NBCs effects on proliferation and lipid metabolism pathways were observed, and the treatments showed different responses, demonstrating distinct ability to interact on metabolic and cell signaling pathways. This may lead to new therapies for the control of infective and inflammatory diseases, such as hepatitis C, which must be evaluated according to the specific application desired, either in the viral replication cycle or in the consequences of the persistence and chronicity of the disease, with the possibility of improvement of current therapeutic schemes.

Funding Sources

This work was supported by the CAPES; FCFAr-UNESP/PADC (Process: 250 - 10/2017) and FAPESP (Process: 2017/04500-9).

Conflicts of Interest

The authors declare that they have no known competing financial interests or personal relationships that could have appeared to influence the work reported in this paper.

Acknowledgements

The authors would like to thank the FCFAr-UNESP/PADC, CAPES and FAPESP for their financial support.

Collaborators

Study design: PIC; RL

Data curation: RL

Data collection: RL

Data analysis: RL; EMR; PIC

Writing of the original manuscript: EMR; LDBT; AMMG; RL; PIC

Writing of the review and editing: EMR; LDBT; AMMG; RL; PIC.

References

1. World Health Orgnization. **Global hepatitis report, 2021**. [http://www.who.who.int/news-room/hepatitits-c,July27,2021/publications/global-hepatitis/en/]. [Accessed: 14 oct 2021].

2. World Health Orgnization. **Hepatitis C (fact sheet)**. [https://www.who.int/news-room/fact-sheets/detail/hepatitis-c]. [Accessed: 09 Mar 2022].

3. Centers for disease control and prevention. **Hepatitis C FAQs for health professionals**. [https://www.cdc.gov/hepatitis/hcv/hcvfaq.htm#section1]. [Accessed: 6 Jun 2021].

4. Gonzalez FA, Van den Eynde E, Perez-Hoyos S, Navarro J, Curran A, Burgos J, *et al*. Liver stiffness and aspartate aminotransferase levels predict the risk for liver fibrosis progression in hepatitis C virus/HIV-coinfected patients. **HIV Med**. 2015; 16: 211-218. [http://dx.doi.org/10.1111/hiv.12197].

5. Pokorska-Śpiewak M, Kowalik-Mikołajewska B, Aniszewska M, Walewska-Zielecka B, Marczyńska M. The influence of hepatitis B and C virus coinfection on liver histopathology in children. **Eur J Pediatr**. 2015; 174: 345-353. [http://dx.doi.org/10.1007/s00431-014-2402-7].

6. Manns MP, Buti M, Gane E, Pawlotsky JM, Razavi H, Terrault N, *et al*. Hepatitis C virus infection. **Nat Rev Dis Primers**. 2017; 3: 17006. [http://dx.doi.org/10.1038/nrdp.2017.6].

7. Biesalski HK, Gragsted LO, Elmadfa I, Grossklaus R, Müller M, Schrenk D, *et al*. Bioactive compounds: Definition and assessment of activity. **Nutrition**. 2009; 25: 1202-1205. [http://dx.doi.org/10.1016/j.nut.2009.04.023].

8. Calland N, Dubuisson J, Rouillé Y, Séron K. Hepatitis C virus and natural compounds: a new antiviral approach? **Viruses** 2012; 4: 2197–2217. [http://dx.doi.org/10.3390/v4102197].

9. Shishodia S, Sethi G, Aggarwal BB. Curcumin: getting back to the roots. **Ann N Y Acad Sci**. 2005; 1056: 206-217. [http://dx.doi.org/10.1196/annals.1352.010].

10. Aggarwal BB, Harikumar KB. Potential therapeutic effects of curcumin, the anti-inflammatory agent, against neurodegenerative, cardiovascular, pulmonary, metabolic, autoimmune and neoplastic diseases. **Int J Biochem Cell Biol**. 2009; 41: 40-59. [http://dx.doi.org/10.1016/j.biocel.2008.06.010].

11. Rechtman MM, Har-Noy O, Bar-Yishay I, Fishman S, Adamovich Y, Shaul Y, *et al*. Curcumin inhibits hepatitis B virus via down-regulation of the metabolic coactivator PGC-1α. **FEBS Lett**. 2010; 584: 2485-2490. [http://dx.doi.org/10.1016/j.febslet.2010.04.067].

12. Anggakusuma, Colpitts CC, Schang LM, Rachmawati H, Frentzen A, Pfaender S, *et al*. Turmeric curcumin inhibits entry of all hepatitis C virus genotypes into human liver cells. **Gut**. 2014; 63: 1137-1149. [http://dx.doi.org/10.1136/gutjnl-2012-304299] .

13. Kumar D, Basu S, Parija L, Rout D, Manna S, Dandapat J, *et al*. Curcumin and ellagic acid synergistically induce ROS generation, DNA damage, p53 accumulation and apoptosis in HeLa cervical carcinoma cells. Biomed. **Pharmacother**. 2016; 81: 31-37. [http://dx.doi.org/10.1016/j.biopha.2016.03.037].

14. Musso G, Cassader M, Gambino R. Non-alcoholic steatohepatitis: emerging molecular targets and therapeutic strategies. **Nat Rev Drug Discov**. 2016; 15: 249-274. [http://dx.doi.org/10.1038/nrd.2015.3].

15. Chen LC, Chen YC, Su CY, Wong WP, Sheu MT, Ho HO. Development and characterization of lecithin-based self-assembling mixed polymeric micellar (saMPMs) drug delivery systems for curcumin. **Sci Rep**. 2016; 6: 37122. [http://dx.doi.org/10.1038/srep37122].

16. Tawani A, Amanullah A, Mishra A, Kumar A. Evidences for piperine inhibiting cancer by targeting human G-quadruplex DNA sequences. **Sci Rep**. 2016; 6: 39239. [http://dx.doi.org/10.1038/srep39239].

17. Lai LH, Fu QH, Liu Y, Jiang K, Guo QM, Chen QY, *et al*. Piperine suppresses tumor growth and metastasis *in vitro* and *in vivo* in a 4T1 murine breast cancer model. **Acta Pharmacol Sin**. 2012; 33: 523–530. [http://dx.doi.org/10.1038/aps.2011.209].

18. Randino R, Grimaldi M, Persico M, De Santis A, Cini E, Cabri W, *et al*. Investigating the neuroprotective effects of turmeric extract: structural interactions of β-amyloid peptide with single curcuminoids. **Sci Rep**. 2016; 6: 38846. [http://dx.doi.org/10.1038/srep38846].

19. Shoba G, Joy D, Joseph T, Majeed M, Rajendran R, Srinivas PS. Influence of piperine on the pharmacokinetics of curcumin in animals and human volunteers. **Pl Med**. 1998; 64: 353-356. [http://dx.doi.org/10.1055/s-2006-957450].

20. Zhou J, Donatelli SS, Gilvary DL, Tejera MM, Eksioglu EA, Chen X, *et al*. Therapeutic targeting of myeloid-derived suppressor cells involves a novel mechanism mediated by clusterin. **Sci Rep**. 2016; 6: 29521. [http://dx.doi.org/10.1038/srep29521].

21. Rieger AM, Nelson KL, Konowalchuk JD, Barreda DR. Modified annexin V/propidium iodide apoptosis assay for accurate assessment of cell death. **J Vis Exp**. 2011; 24(50): 2597. [https://doi.org/10.3791/2597].

22. Xiang J, Wan C, Guo R, Guo D. Is hydrogen peroxide a suitable apoptosis inducer for all cell types? **BioMed Res Int**. 2016; 2016: 7343965. [http://dx.doi.org/10.1155/2016/7343965].

23. **ISO 10993-5 (2005) Biological Evaluation of Medical Devices – Part 5: Tests for *in vitro* cytotoxicity.** Geneva, Switzerland: International Standards Organization, Geneva, Switzerland.

24. Li M, Gao M, Fu Y, Chen C, Meng X, Fan A, Kong D, *et al*. Acetal-linked polymeric prodrug micelles for enhanced curcumin delivery. **Colloids Surf B Biointerfaces**. 2016; 140: 11-18. [http://dx.doi.org/10.1016/j.colsurfb.2015].

25. Jiang J, Jin H, Liu L, Pi J, Yang F, Cai J. Curcumin disturbed cell-cycle distribution of HepG2 cells via cytoskeletal arrangement. **Scanning**. 2013; 35: 253-260. [http://dx.doi.org/10.1002/sca.21058].

26. Prasad NS, Raghavendra R, Lokesh BR, Naidu KA. Spice phenolics inhibit human PMNL-5 lipoxygenase. **Prostaglandins Leukot Essent Fatty Acids**. 2004; 70: 521-528. [http://dx.doi.org/10.1016/j.plefa.2003.11.006].

27. Raghavendra RH, Naidu KA. Spice active principles as the inhibitors of human platelet aggregation and thromboxane biosynthesis. **Prostaglandins Leukot Essent Fatty Acids**. 2009; 81: 73-78. [http://dx.doi.org/0.1016/j.plefa.2009.04.009].

28. Derosa G, Maffioli P, Simental-Mendía LE, Bo S, Sahebkar A. Effect of curcumin on circulating interleukin-6 concentrations A systematic review and meta-analysis of randomized controlled trials. **Pharmacol Res**. 2016; 111: 394-404. [http://dx.doi.org/10.1016/j.phrs.2016.07.004].

29. Rinwa P, Kumar A. Piperine potentiates the protective effects of curcumin against chronic unpredictable stress-induced cognitive impairment and oxidative damage in mice. **Brain Res**. 2012; 1488: 38-50. [http://dx.doi.org/10.1016/j.brainres.2012.10.002].

30. Singh S, Kumar P. Neuroprotective Activity of Curcumin in Combination with Piperine against Quinolinic Acid Induced Neurodegeneration in Rats. **Pharmacology.** 2016; 97: 151-160. [http://dx.doi.org/10.1159/000443896.0].

31. Olmedo E, Costa J, López-Labrador FX, Forns X, Ampurdanés S, Maluenda MD, *et al*. Comparative study of a modified competitive RT-PCR and Amplicor HCV monitor assays for quantitation of hepatitis C virus RNA in serum. **J Med Virol**. 1999; 58: 35-43. [http://dx.doi.org/10.1002/(sici)1096-9071(199905)58:1<35::aid-jmv5>3.0.co;2-v].

32. Elkady A, Tanaka Y, Kurbanov F, Sugauchi F, Sugiyama M, Khan A, *et al*. Performance of two Real-Time RT-PCR assays for quantitation of hepatitis C virus RNA: evaluation on HCV genotypes 1-4. **J Med Virol**. 2010; 82: 1878-888. [http://dx.doi.org/10.1002/jmv.21911].

33. Vrtačnik P, Kos Š, Bustin SA, Marc J, Ostanek B. Influence of trypsinization and alternative procedures for cell preparation before RNA extraction on RNA integrity. **Anal Biochem**. 2014; 463: 38-44. [http://dx.doi.org/10.1016/j.ab.2014.06.017].

34. Kim K, Kim KH, Kim HY, Cho HK, Sakamoto NJ. Cheong. Curcumin inhibits hepatitis C virus replication via suppressing the Akt-SREBP-1 pathway. **FEBS Lett**. 2010; 584: 707-712. [http://dx.doi.org/10.1016/j.febslet.2009.12.019].

35. Chen MH, Lee MY, Chuang JJ, Li YZ, Ning ST, Chen JC, *et al*. Curcumin inhibits HCV replication by induction of heme oxygenase-1 and suppression of AKT. **Int J Mol Med**. 2012; 30: 1021-1028. [https://doi.org/10.3892/ijmm.2012.1096].

36. Assis RP, Arcaro CA, Gutierres VO, Oliveira JO, Costa PI, Bavieira AM, *et al*. Combined effects of curcumin and lycopene or bixin in yoghurt on inhibition of LDL oxidation and increases in HDL and paraoxonase levels in streptozotocin-diabetic rats. **Int J Mol Sci**. 2017; 18: 332. [https://doi.org/10.3390/ijms18040332].

37. Adinolfi LE, Rinaldi L, Guerrera B, Restivo L, Marrone A, Giordano M, *et al*. NAFLD and NASH in HCV infection: prevalence and significance in hepatic and extrahepatic manifestations. **Int J Mol Sci**. 2016; 17: 803. [https://doi.org/10.3390/ijms17060803].

38. Prata TVG, Silva DSRD, Manchiero C, Dantas BP, Mazza CC, Nunes AKDS, *et al*. MTTP polymorphisms and hepatic steatosis in individuals chronically infected with hepatitis C virus. **Arch Virol**. 2019; 164: 2559–2563. [https://doi.org/10.1007/s00705- 019-04352-4].

39. Magri MC, Manchiero C, Prata TVG, Nunes AKDS, Oliveira Junior JS, Dantas BP, *et al*. The influence of gene-chronic hepatitis C virus infection on hepatic fibrosis and steatosis. **Diagn Microbiol Infect Dis**. 2020; 97(2): 115025. [https://doi.org/10.1016/j.diagmicrobio. 2020.115025].

40. Zampino R, Ingrosso D, Durante-Mangoni E, Capasso R, Tripodi MF, Restivo L, *et al*. Microsomal triglyceride transfer protein (MTP) -493G/T gene polymorphism contributes to fat liver accumulation in HCV genotype 3 infected patients. **J Viral Hepat**. 2008; 15: 740-746. [https://doi.org/10.1111/j.1365-2893.2008.00994.x].

41. Cai T, Dufour JF, Muellhaupt B, Gerlach T, Heim M, Moradpour D, *et al*. Viral genotype-specific role of PNPLA3, PPARG, MTTP, and IL28B in hepatitis C virus-associated steatosis. **J Hepatol**. 2011; 55: 529-535. [https://doi.org/10.1016/j.jhep.2010.12.020].

42. Liu Y, Conlon DM, Bi X, Slovik KJ, Shi J, Edelstein HI, Millar JS, *et al*. Lack of MTTP Activity in Pluripotent Stem Cell-Derived Hepatocytes and Cardiomyocytes Abolishes apoB Secretion and Increases Cell Stress. **Cell Rep**. 2017; 19: 1456-1466. [https://doi.org/10.1016/j.celrep.2017.04.064].

43. Winther M, Shpitzen S, Yaacov O, Landau J, Oren L, Foroozan-Rosenberg L, *et al*. In search of a genetic explanation for LDLc variability in an FH family: common SNPs and a rare mutation in *MTTP* explain only part of LDL variability in an FH family. **J Lipid Res**. 2019; 60: 1733-1740. [https://doi.org/10.1194/jlr.M092049].

44. Ellis KL, Hooper AJ, Burnett JR, GF Watts. Progress in the care of common inherited atherogenic disorders of apolipoprotein B metabolism. **Nat Rev Endocrinol**. 2016; 12: 467-484. [https://doi.org/10.1038/nrendo.2016.69].

45. Charlton-Menys V, Durrington PN. Human cholesterol metabolism and therapeutic molecules. **Exp Physiol**. 2008; 93: 27-42. [https://doi.org/10.1113/expphysiol.2007.035147].

46. Parhofer KG. The treatment of disorders of lipid metabolism. **Dtsch Arztebl Int**. 2016; 113: 262-268. [https://doi.org/10.3238/arztebl.2016.0261].

47. Crowley LC, Marfell BJ, Scott AP, Waterhouse NJ. Quantitation of apoptosis and necrosis by annexin V binding, propidium iodide uptake, and flow cytometry. **Cold Spring Harb Protoc**. 2016; 2016:. [https://doi.org/10.1101/pdb.prot087288].

48. Aggarwal BB, Deb L, Prasad S. Curcumin differs from tetrahydrocurcumin for molecular targets, signaling pathways and cellular responses. **Molecules** 2015; 20: 185-205. [https://doi.org/10.3390/molecules20010185].

49. J Wang, Wang C, Bu G. Curcumin inhibits the growth of liver cancer stem cells through the phosphatidylinositol 3-kinase/protein kinase B/mammalian target of rapamycin signaling pathway. **Exp Ther Med**. 2018; 15: 3650-3658. [https://doi.org/10.3892/etm.2018.5805].

50. Shiu TY, Huang SM, Shih YL, Chu HC, Chang WK, Hsieh TY. Hepatitis C virus core protein down-regulates p21Waf1/Cip1 and inhibits curcumin-induced apoptosis through microRNA-345 targeting in human hepatoma cells. **PLoS One**. 2017; 12: e0181299. [https://doi.org/10.1371/journal.pone.0181299].

51. Wu LY, Chen CW, Chen LK, Chou HY, Chang CL, Juan CC. Curcumin Attenuates Adipogenesis by Inducing Preadipocyte Apoptosis and Inhibiting Adipocyte Differentiation. **Nutrients**. 2019; 11: 2307. [https://doi.org/10.3390/nu11102307].

52. Han SZ, Liu HX, Yang LQ, Cui LD, Xu Y. Piperine (PP) enhanced mitomycin-C (MMC) therapy of human cervical cancer through suppressing bcl-2 signaling pathway via inactivating STAT3/NF-κB. **Biomed Pharmacother**. 2017; 96: 1403-1410. [https://doi.org/10.1016/j.biopha.2017.11.022].

53. Lin Y, Xu J, Liao H, Li L, Pan L. Piperine induces apoptosis of lung cancer A549 cells via p53-dependent mitochondrial signaling pathway. **Tumour Biol** 35(2014) 3305-10. [https://doi.org/10.1007/s13277-013-1433-4].

54. Gunasekaran V, Elangovan K, Niranjali Devaraj S. Targeting hepatocellular carcinoma with piperine by radical-mediated mitochondrial pathway of apoptosis: An *in vitro* and *in vivo* study. **Food Chem Toxicol**. 2017; 105: 106-118. [https://doi.org/10.1016/j.fct.2017.03.029].

55. Tikhanovich I, Kuravi S, Campbell RV, Kharbanda KK, Artigues A, Villar MT, *et al*. Regulation of FOXO3 by phosphorylation and methylation in hepatitis C virus infection and alcohol exposure. **Hepatology**. 2014; 59(1): 58-70. [https://doi.org/10.1002/hep.26618].

56. Tikhanovich I, Cox J, Weinman SA. Forkhead box class O transcription factors in liver function and disease. **J Gastroenterol Hepatol**. 2013; 28: 125-131. [https://doi.org/10.1111/jgh.12021].

57. Herzig S, Shaw RJ. AMPK: guardian of metabolism and mitochondrial homeostasis. **Nat Rev Mol Cell Biol**. 2018; 19: 121-135. [https://doi.org/10.1038/nrm.2017.95].

58. Mankouri J, Tedbury PR, Gretton S, Hughes ME, Griffin SD, Dallas ML, *et al*. Enhanced hepatitis C virus genome replication and lipid accumulation mediated by inhibition of AMP-activated protein kinase. **Proc Natl Acad Sci U S *A***. 2010; 107(25): 11549–11554. [https://doi.org/10.1073/pnas.0912426107].

59. Liu Z, Cui C, Xu P, Dang R, Cai H, Liao D, *et al*. Curcumin activates AMPK pathway and regulates lipid metabolism in rats following prolonged clozapine exposure. **Front Neurosci**. 2017; 11: 558. [https://doi.org/10.3389/fnins.2017.00558].

60. Seren S, M Mutchnick, Hutchinson D, Harmanci O, Bayraktar Y, Mutchnick S, *et al*. Potential role of lycopene in the treatment of hepatitis C and prevention of hepatocellular carcinoma. **Nutr Cancer**. 2008; 60(6): 729-735. Disponível em: [https://doi.org/10.1080/01635580802419772] .

61. Dolka I, Król M, Sapierzyński R. Evaluation of apoptosis-associated protein (Bcl-2, Bax, cleaved caspase-3 and p53) expression in canine mammary tumors: an immunohistochemical and prognostic study. **Res Vet Sci**. 2016; 105: 124-133. [http://dx.doi.org/10.1016/j.rvsc.2016.02.004].

62. Salakou S, Kardamakis D, Tsamandas AC, Zolota V, Apostolakis E, V Tzelepi, *et al*. Increased bax/bcl-2 ratio up-regulates caspase-3 and increases apoptosis in the thymus of patients with *Myasthenia gravis*. ***In Vivo***. 2007; 21(1): 123-132. [https://pubmed.ncbi.nlm.nih.gov/17354625/].

63. Masalova OV, Lesnova EI, Solyev PN, Zakirova NF, Prassolov VS, Kochetkov SN, *et al*. Modulation of cell death pathways by hepatitis C virus proteins in Huh7.5 hepatoma cells. **Int J Mol Sci**. 2017; 18(11): 2346. [https://doi.org/10.3390/ijms18112346].

64. Pal MK, Jaiswar SP, Srivastav AK, Goyal S, Dwivedi A, Verma A, *et al*. Synergistic effect of piperine and paclitaxel on cell fate via cyt-c, bax/bcl-2-caspase-3 pathway in ovarian adenocarcinomas SKOV-3 cells. **Eur J Pharmacol**. 2016; 791: 751–762. [http://dx.doi.org/10.1016/j.ejphar.2016.10.019].

65. Manning BD, Toker A. AKT/PKB signaling: navigating the network. **Cell**. 2017; 169: 381-405. [https://doi.org/10.1016/j.cell.2017.04.001].

66. Liu Z, Tian Y, Machida K, Lai MM, Luo G, Foung SK, Ou JH. Transient activation of the PI3K-AKT pathway by hepatitis C virus to enhance viral entry. **J Biol Chem**. 2012; 287: 41922-41930. [https://doi.org/10.1074/jbc.M112.414789].

67. Shi Q, Hoffman B, Liu Q. PI3K-Akt signaling pathway upregulates hepatitis C virus RNA translation through the activation of SREBPs. **Virology**. 2016; 490: 99-108. [https://doi.org/10.1016/j.virol.2016.01.012].

68. Zhao Y, Hu X, Liu Y, Dong S, Wen Z, He W, *et al*. ROS signaling under metabolic stress: cross-talk between AMPK and AKT pathway. **Mol Cancer**. 2017; 16: 79. [https://doi.org/10.1186/s12943-017-0648-1].

Histórico do artigo | Submissão: 14/12/2024 | **Aceite:** 05/02/2025

Como citar este artigo: Lopes R, Toledo LDB, Rodrigues EM, Gaspar AMM, *et al*. Mechanistic insights into the antiviral effects of curcumin and piperine against Hepatitis C virus: a study of their bioactive properties in hepatocarcinoma cells. **Rev Fitos**. Rio de Janeiro. 2025; 19(1): e1813. e-ISSN 2446.4775. Disponível em: <https://doi.org/10.32712/2446-4775.2025.1813>. Acesso em: dd/mm/aaaa.